The Protective Effect of Functional Connexin43 Channels on a Human Epithelial Cell Line Exposed to Oxidative Stress

Cindy M. L. Hutnik,[1] *Cady E. Pocrnich,*[1] *Hong Liu,*[1] *Dale W. Laird,*[2] *and Qing Shao*[2]

Purpose. To determine the role of connexin43 (Cx43) and gap junctional intercellular communication (GJIC) in the response of the human retinal pigment epithelial cell line ARPE-19 to oxidative stress.

Methods. ARPE-19 cells were treated with the chemical oxidant *tert*-butyl hydroperoxide (t-BOOH), and cell viability was assessed by the MTT [3-(4,5-dimethylthiazol-2-yl)-2,5-diphenyltetrazolium bromide] assay. GJIC was evaluated by scrape loading/dye transfer and microinjection assays, and Cx43 expression was detected by Western blot and immunofluorescent staining combined with confocal microscopy analysis. Retroviral infection of ARPE-19 cells with shRNA vectors targeting Cx43 or vectors encoding Cx43, Cx26, and a disease-linked dominant negative Cx43 mutant (G21R) were used, and the effect on cell viability was assessed.

Results. t-BOOH–induced ARPE-19 cell death was correlated with reductions in GJIC and in the total level of Cx43 protein expression. Overexpression of Cx26 and Cx43 increased the viability of oxidant-treated ARPE-19 cells. Conversely, shRNA knockdown of Cx43, expression of a disease-linked dominant negative Cx43 mutant, and blocking GJIC with 18β-glycyrrhetinic acid and flufenamic acid all increased t-BOOH–induced ARPE-19 cell death.

Conclusions. Cx43-mediated protection of ARPE-19 cells from oxidative stress-induced death is dependent on functional Cx43 channels. (*Invest Ophthalmol Vis Sci.* 2008;49:800–806) DOI:10.1167/iovs.07-0717

Age-related macular degeneration (AMD) is a leading cause of visual impairment in the Western world[1–3] and is characterized by progressive loss of photoreceptors in the central retina secondary to dysfunction of the retinal pigment epithelium (RPE).[4] Although the etiology of AMD has been attributed to many environmental, nutritional, behavioral, and genetic factors,[5] advancing age remains the strongest disease risk factor.[6] Oxidative stress with impaired free radical scavenging is known to be a fundamental mechanism of aging.[7] Loss of integrity of the RPE is known to be a fundamental early event in AMD.[4]

Oxidative stress refers to the harmful interactions of reactive oxygen species (ROS) with cellular components occurring when ROS production exceeds the ability of antioxidant systems to mitigate damage. The RPE produces considerable amounts of ROS. The high rate of oxygen consumption by the retina creates oxidative load,[8] as does RPE phagocytosis of spent photoreceptor outer segments rich in polyunsaturated fatty acids.[8,9] Exposure to light induces chromophores in the RPE and surrounding tissues to generate ROS.[10,11] These factors make the RPE particularly susceptible to oxidative stress, providing motivation to characterize the RPE cellular response to oxidative stress. To do this, many researchers have established toxicity models in which stressors known to cause oxidative damage are applied to RPE cell lines. Results of two such studies showed that RPE cells in suspension are more sensitive to the chemical oxidant *tert*-butyl hydroperoxide (t-BOOH) than those cells not in suspension.[5,12,13] This suggests the possibility that cell-cell contact may promote a favorable RPE response to oxidative stress.

Complexes that mediate cell-cell contact, and hence monolayer integrity, include tight junctions, adherens junctions, and gap junctions. Oxidative stress is known to disrupt the integrity of RPE tight junctions, and this may contribute to blood-retinal barrier breakdown.[14] The effect of oxidative stress on gap junctions and, conversely, the effect of gap junctions on the RPE response to oxidative stress have not been explored. Gap junction channels consist of two juxtaposed hemichannels, one from each adjacent cell, that allow for the intercellular exchange of small signaling molecules (<1 kDa).[15] The basic units of hemichannels are connexin proteins. The human connexin family consists of 21 connexins, with connexin43 (Cx43) the most widely expressed across tissue types. Gap junctional intercellular communication (GJIC) has been implicated in several cell types in response to various stressors, including hydrogen peroxide,[16] radiation,[17] and ultraviolet light.[18] The role of GJIC in the oxidant-stressed RPE has not yet been characterized.

The present study was performed to examine the role(s) of Cx43 and GJIC in an oxidatively stressed ARPE-19 cell line. Our findings suggest that Cx43-mediated protection of ARPE-19 cells from oxidative stress-induced death is dependent on functional Cx43 channels.

Materials and Methods

Reagents

All cell culture reagents were purchased from Invitrogen (Gibco BRL, Burlington, ON, Canada), unless otherwise indicated. Antibodies were purchased from New England Biolabs (Mississauga, ON, Canada). MTT and t-BOOH were purchased from Sigma-Aldrich (Oakville, ON, Canada).

ARPE-19 Cell Culture

The human retinal pigment epithelial cell line ARPE-19 was purchased from American Type Culture Collection (Manassas, VA). ARPE-19 cells within 10 passages from the time of purchase were cultured in a 1:1 mixture of Dulbecco modified Eagle Medium (Invitrogen-Life Technol-

From the Departments of [1]Ophthalmology and [2]Anatomy and Cell Biology, University of Western Ontario, London, Ontario, Canada.

Submitted for publication June 14, 2007; revised September 29, 2007; accepted December 17, 2007.

Disclosure: **C.M.L. Hutnik**, None; **C.E. Pocrnich**, None; **H. Liu**, None; **D.W. Laird**, None; **Q. Shao**, None

The publication costs of this article were defrayed in part by page charge payment. This article must therefore be marked "*advertisement*" in accordance with 18 U.S.C. §1734 solely to indicate this fact.

Corresponding author: Cindy M. L. Hutnik, St. Joseph's Health Care London, 268 Grosvenor Street, London, Ontario, Canada N6A 4V2; cindyh@sjhc.london.on.ca.

ogy, Rockville, MD) and Ham F12 (DMEM/F12) containing 10% fetal bovine serum (FBS) and 1% penicillin-streptomycin, at 37°C in 5% CO_2.

Constructs and Retroviral Infection

Engineering of Cx43-green fluorescent protein (Cx43-GFP) and Cx26-green fluorescent protein (Cx26-GFP) was described previously.[19–21] The disease-linked dominant negative human Cx43 mutant, G21R, is described elsewhere.[22] Three recombinant retroviral vectors (Cx43-GFP, Cx26-GFP, and G21R-GFP) and an empty vector were transfected into the 293 GPG retroviral packaging cell line. A replication-defective virus-containing supernatant was produced, and retroviral infection of ARPE-19 cells was performed as described.[23] In each instance, fluorescent analysis revealed that more than 90% of the cells expressed the recombinant connexins.

RNAi knockdown of Cx43 was performed as described.[24] The target sequence 5′-GAAGTTCAAGTACGGGATT-3′ of Cx43 was cloned into a replication-incompetent pH1.1-QCXIH retroviral vector. The insert-containing retroviral vector was transfected into HEK293 packaging cells (BD Biosciences, Mississauga, ON, Canada) using reagent (Lipofectamine 2000; Invitrogen) to generate infectious viral particle-containing supernatant. We used empty retroviral vector and the nonsense sequence 5′-AATTCTCCGAACGTGTCACGT-3′ as the RNAi control group for our experiments. ARPE-19 cells were infected and selected in 50 μg/mL hygromycin medium and were subcultured at least five times to ensure that a stable cell line was obtained. Western blot was used to confirm the downregulation of Cx43 protein before additional experiments.

t-BOOH Treatment

ARPE-19 cells were seeded at 3×10^4 cells/cm^2 onto 96-well plates or 60-mm dishes and grown for 48 hours to 100% confluence. The cells were untreated or treated with 1 to 5 mM t-BOOH (Sigma, St. Louis, MO) for up to 4 hours as required in the culture media.

Dye Transfer Assays

GJIC was assessed using the scrape loading/dye transfer assay.[25] Briefly, ARPE-19 cells were grown to 100% confluence in 60-mm dishes. After medium was removed, cells were scraped with a surgical blade, and Lucifer yellow (1 mg/mL; Molecular Probes, Eugene, OR) dissolved in PBS was added immediately. Five minutes later, the cells were washed with PBS to remove excess dye and were fixed with 3.7% formalin. A fluorescence microscope was used to view Lucifer yellow-positive cells, and dye spread was defined as the distance of Lucifer yellow-positive cells from the scrape line.

For other studies, a microinjection assay was used to assess GJIC.[22] Cells were pressure microinjected with 5% Lucifer yellow using an automated pressure microinjector (FemtoJet; Eppendorf, Westbury, NY), and the percentage of microinjected cells that transferred Lucifer yellow to neighboring cells was determined. Cells were visualized with an inverted epifluorescent microscope (DM IRE2; Leica, Wetzlar, Germany). Approximately 1 to 4 minutes after microinjection, digital images were collected with a charge-coupled device camera (Hamamatsu Photonics, Hamamatsu, Japan) using scientific imaging software (OpenLab; Improvision, Waltham, MA). The percentage of microinjected cells that exhibited dye coupling was determined as previously described.[26]

MTT Assay

The MTT reduction assay was used as an index of cell viability and was performed according to the manufacturer's instructions. Briefly, control and t-BOOH– treated ARPE-19 cells were incubated in serum-free medium containing 0.4 mg/mL MTT [3-(4,5-dimethylthiazol-2-yl)-2,5-diphenyltetrazolium bromide]. During this time, mitochondrial and cytosolic dehydrogenases of living cells reduced the yellow tetrazolium salt (MTT) to a purple formazan dye capable of spectrophotometric detection. After 2 to 2.5 hours, the MTT solution was aspirated and dimethylsulfoxide (0.3 mL/well) was added. Optical densities of the supernatant were read at 575 nm using a microplate spectrophotometer (Spectra Max 340; Molecular Devices, Sunnyvale, CA). Absorbances were normalized to the untreated control cultures, which represented 100% viability.

Immunocytochemistry

Immunofluorescent labeling and imaging was performed as previously described.[27] Briefly, cells grown on 12-mm glass coverslips were fixed with 80% methanol/20% acetone at 4°C for 15 minutes. Cells were labeled with a 1:500 dilution of a polyclonal anti-Cx43 antibody (Sigma-Aldrich). After several washings, cells were incubated for 1 hour with donkey anti-rabbit antibody conjugated to Texas red (Jackson ImmunoResearch Laboratories, West Grove, PA). Coverslips were rinsed with distilled water, mounted, and analyzed with a confocal microscope (LSM 510 META; Zeiss, Thornwood, NY) equipped with a 63× oil (1.4 NA) objective. Fluorescent signals were imaged after excitation with 543-nm or 730-nm laser lines produced by a helium-neon or tunable multiphoton lasers (Chameleon; Coherent, Santa Clara, CA), respectively. All fluorescent signals were collected on a photomultiplier after passage through appropriate filter sets. Digital images were prepared using appropriate software (Zeiss LSM, Adobe Photoshop 7.0, or Core Draw 10).

Protein Extraction and Western Blot Analysis

Protein was isolated from confluent ARPE-19 cells growing on 10-cm dishes by washing in PBS at 4°C and then adding lysis buffer (50 mM Tris-HCl [pH 8], 150 mM NaCl, 0.02% N_3Na, 100 μg/mL phenylmethylsulfonyl fluoride, 1% NP-40, 50 mM NaF, 2 mM EDTA, and protease inhibitor [Roche Diagnostics, Laval, Quebec, QC, Canada]). Cell lysates were collected as previously described.[28] Reducing SDS-PAGE and Western blotting was performed as previously described.[27] The blots were labeled with anti-Cx43 antibody (Sigma-Aldrich, St. Louis, MO) at a dilution of 1:10,000. The membranes were washed and then incubated with anti–rabbit horseradish peroxidase-conjugated secondary antibody (1:10,000). Detection was performed using the enhanced chemiluminescence method (Pierce Biotechnology, Rockford, IL). To ensure equal protein loading, nitrocellulose membranes were stripped (REblot; Chemicon International, Temecula, CA) and reprobed with anti–GAPDH antibody at a dilution of 1:10,000 (Cedarlane Laboratories, Hornby, ON, Canada).

Statistical Analysis

All data are given as the mean ± SD of at least three experiments. Where applicable, differences between two groups were compared by the unpaired Student's *t*-test. For multigroup comparisons, ANOVA followed by Student-Newman-Keuls test was performed. $P < 0.05$ was considered statistically significant.

Results

t-BOOH Induced ARPE-19 Cell Death

The chemical oxidant t-BOOH has rapid membrane permeability and can disrupt mitochondrial membrane potentials of treated cells.[29] In the present study, we used t-BOOH as an in vitro model of oxidative stress. Figure 1 shows that t-BOOH induced ARPE-19 cell death in a time-dependent (A) and a dose-dependent (B) manner, as assessed by the MTT assay. A 3-mM dose of t-BOOH decreased cell viability by 17% (2.5 hours), 37% (3.5 hours), and 79% (4 hours) (Fig. 1A). A 3.5-hour incubation with t-BOOH decreased cell viability by 20% (1 mM), 37% (3 mM), and 54% (5 mM) (Fig. 1B). To optimize our ability to examine any potentially protective effects of Cx43 and GJIC, the dose and time combination (3 mM, 3.5 hours) producing approximately 60% viability was chosen for subsequent experiments.

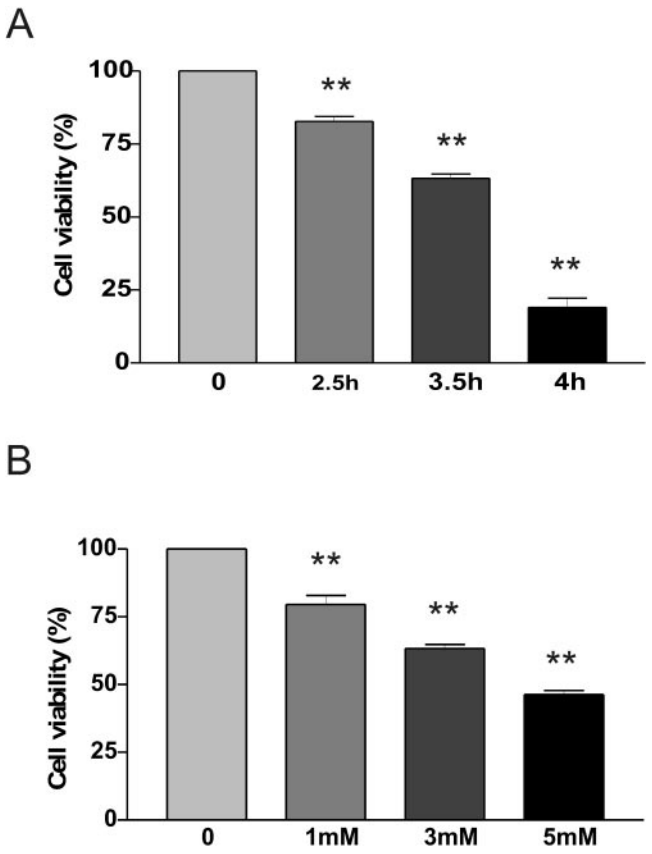

FIGURE 1. Viability of ARPE-19 cells after t-BOOH treatment. Cells were cultured in 96-well plates at a density of 1×10^4 cells/well. (**A**) Cells were treated with 3 mM t-BOOH for 0, 2.5, 3.5, and 4 hours, and cell viability was assessed by the MTT assay. (**B**) Cells were treated with increasing concentrations of t-BOOH for 3.5 hours, and cell viability was assessed by the MTT assay. *Asterisks*: statistical significance from control ($^{**}P < 0.05$; $n = 4$).

t-BOOH Reduced Cx43 Expression and Altered Cx43 Intracellular Distribution in ARPE-19 Cells

Cx43 expression in control and oxidant-stressed cells was assessed by Western blot. Figures 2A and 2B reveal that treatment with t-BOOH for 1, 2, and 3.5 hours caused a decrease in the overall expression of Cx43 monomeric protein. Oxidative stress was also associated with the appearance of a higher molecular weight band, suggestive of an aggregated form of Cx43 (Fig. 2A). Cx43 exists in varying states of phosphorylation, and Cx43 phosphorylation status can be detected by Western blot as bands separated according to degree of phosphorylation. The band P0 represents the least phosphorylated species of Cx43. Densitometric analysis revealed that the decrease in P0 species intensity preceded the decrease in total Cx43 at 1 hour (Fig. 2B). At 3.5 hours, reductions of approximately 40% in total Cx43 and approximately 50% in the P0 species of Cx43 were observed (Fig. 2B).

The distribution pattern of Cx43 in control and oxidant stressed cells was determined by immunocytochemistry in conjunction with confocal microscopy. In both cases, Cx43 was localized to the plasma membranes at zones of cell-cell contract (Fig. 2C). However, perinuclear Cx43 was more qualitatively evident in t-BOOH–treated cells than in control cells. Collectively, these studies suggest that oxidative stress reduces the levels of Cx43 while partially altering the Cx43 distribution pattern.

t-BOOH Treatment Reduced GJIC in hRPE Cells

A scrape loading/dye transfer assay was used to determine whether the reduction of Cx43 protein levels resulted in reduced GJIC. Figure 3A shows that t-BOOH treatment reduced the distance of dye migration from the scrape line. This effect was time dependent (Fig. 3B). In a separate assessment of GJIC, control and t-BOOH–treated cells were microinjected with Lucifer yellow to assess the incidence of dye transfer. In ARPE-19 cells treated with t-BOOH, only 60% (12/20) of microinjected cells transferred dye to neighboring cells, and in those cases, dye spread was restricted to first-order cells. In contrast, dye from 100% of the microinjected control cells (8/8) spread extensively to second and third cells, indicative of excellent GJIC (data not shown).

Overexpression of Cx43 and Cx26 Attenuated t-BOOH–Induced ARPE-19 Cell Death

To examine whether connexins have some effect in protecting ARPE-19 cells from oxidant-induced cell death, populations of cells were generated that overexpressed Cx43 or Cx26. As shown in Figure 4, overexpression of Cx43 or Cx26 reduced

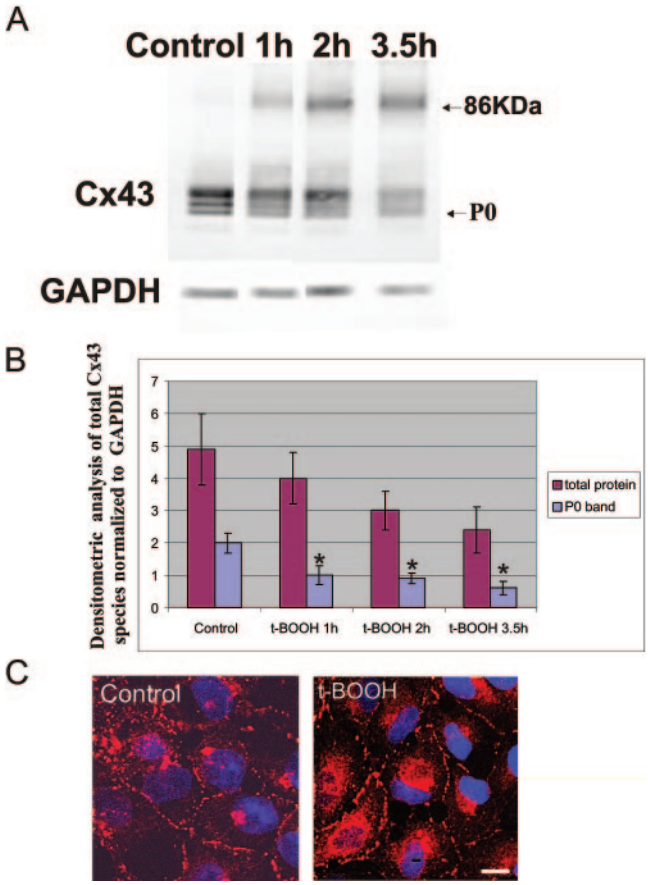

FIGURE 2. t-BOOH reduced Cx43 protein expression in ARPE-19 cells. (**A**) Cells were treated with t-BOOH for 1, 2, or 3.5 hours before cell lysates were probed by Western blot for Cx43 or GAPDH expression. Monomeric dimer and an apparent Cx43 dimer (*arrow*) were detected, with the presence of the dimer increasing in intensity on t-BOOH treatment. (**B**) Densitometric analysis was used to quantify the total expression level of Cx43 (all monomeric species), normalized to GAPDH. *Asterisks*: statistical significance from control ($^{*}P < 0.01$; $n \geq 4$). (**C**) Cells treated with t-BOOH for 3.5 hours were fixed and immunolabeled for Cx43. Scale bar, 10 μm.

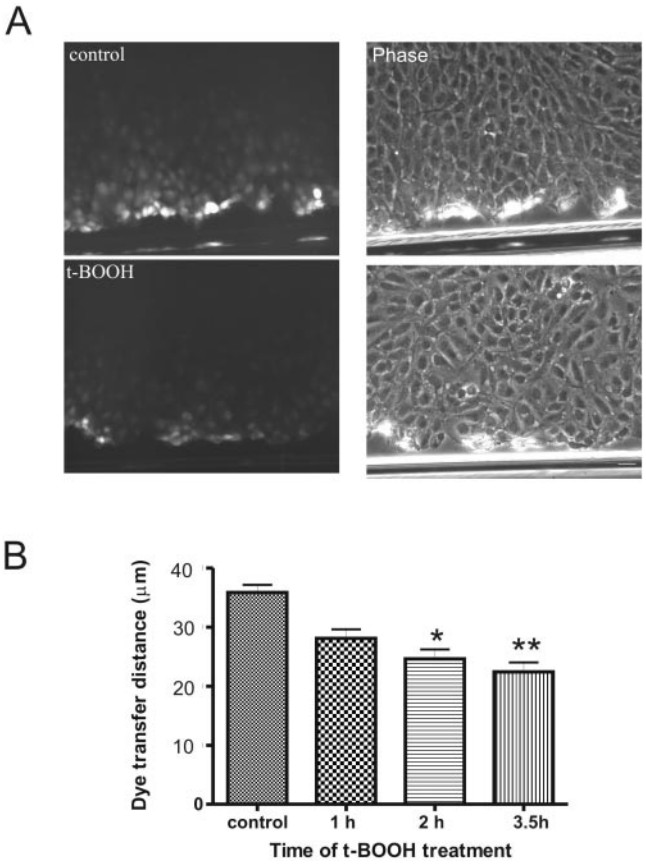

FIGURE 3. t-BOOH inhibited GJIC. ARPE-19 cells were grown on 60-mm culture dishes to 100% confluence before treatment with 3 mM t-BOOH for 1, 2, or 3.5 hours. Untreated and treated cells were scrape-loaded with Lucifer yellow dye (**A**), and dye migration from the scraped edge was measured (**B**). t-BOOH treatment statistically inhibited dye transfer after 2 hours ($^*P < 0.05$; $n = 3$) and 3.5 hours ($^{**}P < 0.01$; $n = 3$). Scale bar, 50 μM.

t-BOOH–induced cell death, suggesting that high expression levels of at least two members of the connexin family serve to protect ARPE-19 cells against the toxic effects of oxidative stress.

Reduced Expression of Cx43 Enhanced t-BOOH–Induced hRPE Cell Death

Because the overexpression of Cx43 and Cx26 was shown to attenuate t-BOOH–induced cell death, we hypothesized that Cx43 knockdown would sensitize the cells to t-BOOH challenge. To test this hypothesis, a retroviral approach was used to knock down Cx43 by as much as 80% in ARPE-19 cells, as assessed by Western blot (Fig. 5A) and immunofluorescent labeling (Fig. 5B). Cells with reduced Cx43 were found to be more sensitive to t-BOOH–induced cell death, as assessed by the MTT assay (Fig. 5C).

Reduced GJIC Enhanced t-BOOH–Induced ARPE-19 Cell Death

Cx43 overexpression and knockdown experiments have suggested a protective role for Cx43 against t-BOOH–induced cell death. To determine whether this protective role was dependent merely on Cx43 expression or whether functional gap junction channels were required, a stable ARPE-19 cell line was established that expressed the disease-linked dominant negative Cx43 mutant (G21R-GFP). Western blot analysis revealed that G21R-GFP fusion protein was expressed (Fig. 6A). We previously showed that this mutant not only was nonfunctional but was dominant-negative to the function of coexpressed endogenous Cx43.[21] The G21R-GFP–expressing ARPE-19 cell line displayed increased susceptibility to t-BOOH–induced cell death compared with an empty vector control (Fig. 6B). These data suggest that the reduction in GJIC induced by the expression of the Cx43 mutant increased the sensitivity of the cells to oxidative damage.

To further test the importance of functional GJIC, we blocked GJIC in oxidant-stressed ARPE-19 cells using the drug blockers 18β-glycyrrhetinic acid (GZA) and flufenamic acid (FFA). GZA facilitates disassembly of gap junction plaques[30] and FFA blocks gap junctions as well as a wide variety of other channels.[31–33] Neither blocker is known to affect connexin expression. Both blockers reduced functional GJIC, as assessed by dye transfer assays (data not shown). GZA (0.1 mM), FFA (50 nM), or vehicle was applied to ARPE-19 cultures for 30 minutes, followed by treatment with 3 mM t-BOOH for 3.5 hours. Cell cultures treated with gap junction blockers exhibited more cell death than cultured cells treated only with vehicle (Fig. 6C), suggesting that functional GJIC protects against the toxic effects of oxidative stress. In the absence of t-BOOH, the gap junction inhibitors did not have an appreciable effect on cell viability when used at these concentrations and time periods.

DISCUSSION

The maintenance of retinal homeostasis by the RPE is essential for the preservation of normal vision. The RPE is a known target of injury in AMD. Although many factors likely contribute to the demise of the RPE in this condition, oxidative stress mismanagement coincident with increasing age may be of importance.[4,5,8] The role of oxidative stress in RPE monolayer disruption at the level of gap junctions is the focus of this report. The disease process of AMD is difficult to reproduce in vitro because damage to the RPE may be accrued over decades and the causes of RPE cell death are multifactorial.[8,34] Other investigators have used acute challenges of the chemical oxidant t-BOOH to RPE cell lines as an approximation of the oxidative damage to the RPE occurring in AMD.[12,13,35] For the present study, this model was adopted to characterize the relationship(s) between oxidative stress, connexin expression, GJIC, and cell viability in an ARPE-19 human RPE cell line.

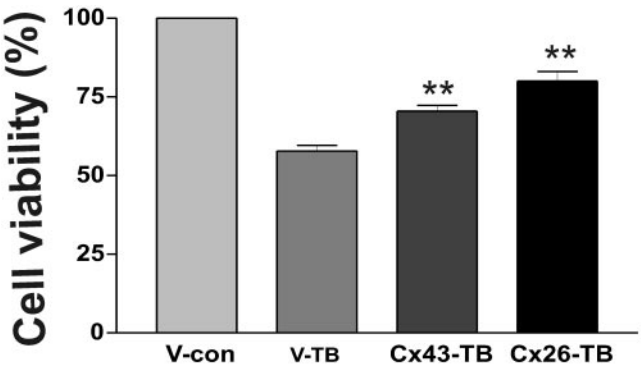

FIGURE 4. Cx43 and Cx26 overexpression protected ARPE-19 cells from oxidant-induced cell death. ARPE-19 cells overexpressing Cx43 or Cx26 or infected with a retroviral empty control vector (V-con) were challenged with 3 mM t-BOOH (TB) for 3.5 hours. Cell viability was assessed by the MTT assay. Overexpression of Cx43 and Cx26 attenuated t-BOOH–induced cell death compared with control retroviral infection cultures (V-TB; $^{**}P < 0.01$; $n = 4$).

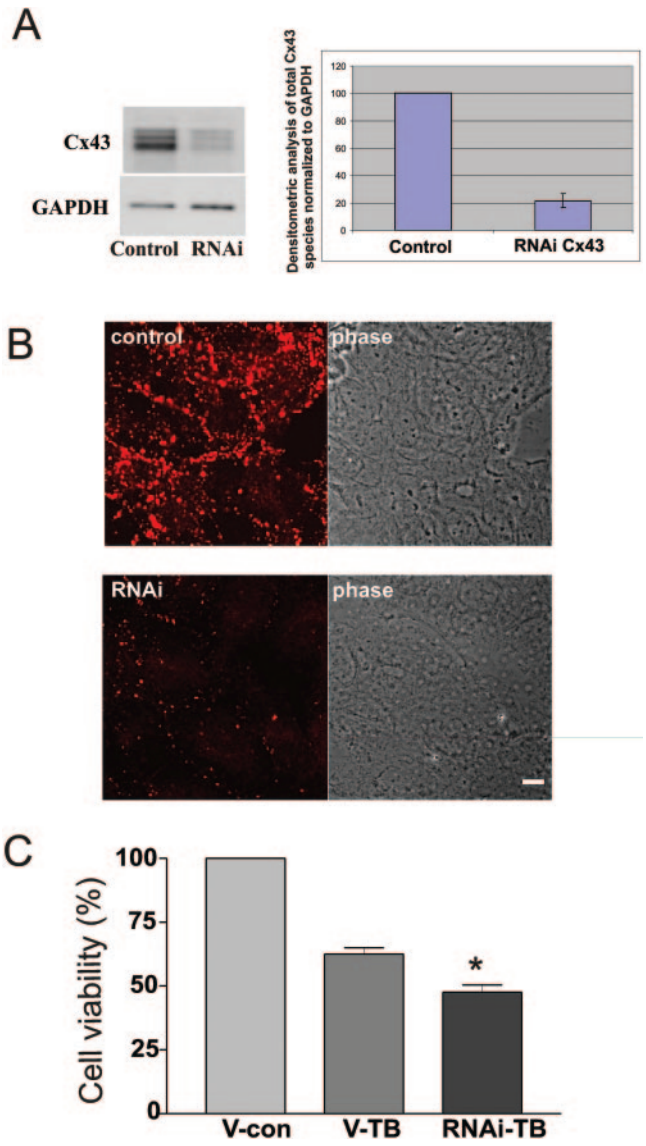

FIGURE 5. Cx43 knockdown enhanced t-BOOH–induced ARPE-19 cell death. (**A**) Western blot and densitometric analysis revealed that RNAi treatment reduced Cx43 levels by approximately 80% ($n = 4$). (**B**) Immunolabeling for Cx43 revealed a reduction in Cx43 staining in RNAi treated cells compared with control cells. Scale bar, 10 μm. (**C**) ARPE-19 cells with knocked down Cx43 were more sensitive to treatment with 3 mM t-BOOH for 3.5 hours, as assessed by the MTT assay ($^*P < 0.01$; $n = 4$).

Given that Cx43 is the most widely expressed connexin and has been identified in RPE cells,[36] experiments with Cx43 were performed.

The results showed that a t-BOOH challenge reduced the expression of Cx43 in ARPE-19 cells. Reduction of the P0 species preceded the reduction of total Cx43, suggesting that the most highly phosphorylated species of Cx43, which are indicative of gap junction plaques,[36] were less susceptible to the effects of oxidative stress than the P0 species typically found within intracellular compartments. In addition, the oxidant-induced reduction of monomeric Cx43 was associated with the concomitant appearance of a high molecular weight species suggestive of Cx43 dimerization or aggregation. It is plausible that oxidative stress causes the P0 species of Cx43 to aggregate into nonfunctional dimers while the more highly phosphorylated forms of Cx43 are left relatively unaffected. The increase in perinuclear Cx43 localization in oxidant-treated cells is consistent with the hypothesis that oxidative stress induces intracellular aggregation of Cx43. However, this hypothesis remains to be explored more comprehensively in a future study. Interestingly, and as may be expected, the reduction in total Cx43 correlated well with a reduction in GJIC because less Cx43 was available for the assembly of functional gap junction channels.

Initial experiments revealed reductions in Cx43 expression, GJIC, and cell viability on t-BOOH exposure. Therefore, levels of Cx43 protein or GJIC, or of both, were enhanced to determine whether the viability of oxidatively stressed cells could be improved. Overexpression of Cx43 improved ARPE-19 viability on t-BOOH exposure, suggesting a potential protective role for this connexin in the oxidant-stressed cells. The mechanisms by which Cx43 may exert its protective effect against oxidative stress fall into two broad categories. First, Cx43 subunits may assemble into functional gap junction channels

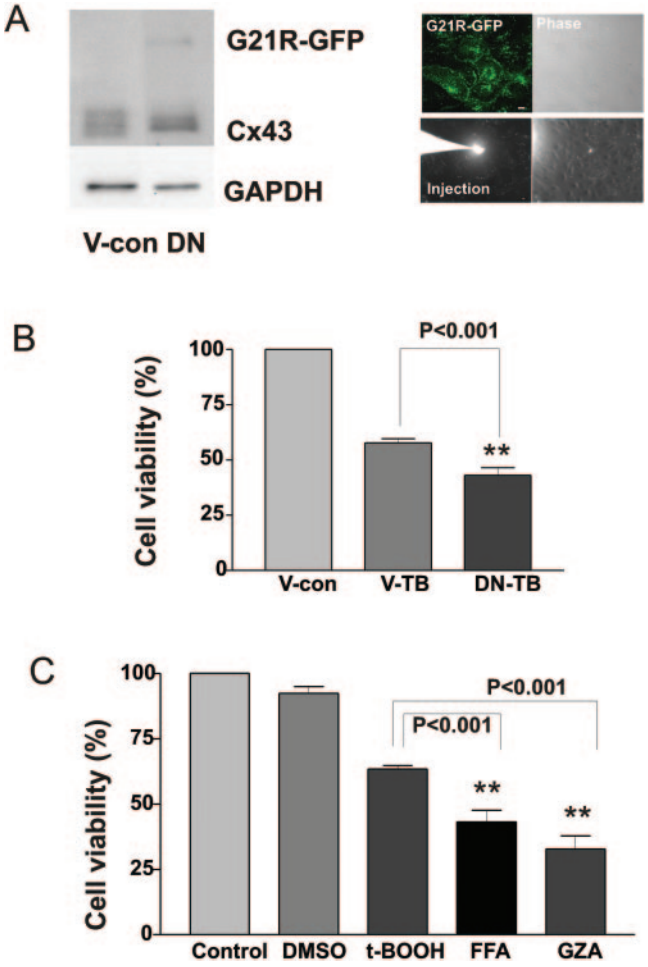

FIGURE 6. Expression of a dominant-negative Cx43 mutant and gap junction blockers facilitated t-BOOH–induced ARPE-19 cell death. (**A**) Western blot analysis for Cx43 and GAPDH in control cells (V-con) and in cells expressing a dominant-negative (DN) Cx43 mutant, G21R-GFP. Fluorescence microscopy of mutant-expressing cells revealed that more than 90% of the cells expressed the mutant. Dye microinjection studies revealed that mutant-expressing cells did not communicate through gap junctions. Scale bar, 10 μm. (**B**) Expression of the G21R-GFP mutant significantly increased t-BOOH (TB)–induced cell death ($^{**}P < 0.001$; $n = 12$). (**C**) Similarly, when gap junctional intercellular communication was blocked with 0.1 mM 18β-glycyrrhetinic acid (GZA) or 50 nM flufenamic acid (FFA) for 30 minutes, t-BOOH–induced cell death was significantly increased ($^{**}P < 0.001$; $n = 5$).

permitting coordinated and regulated GJIC. Alternatively, Cx43 expression may modulate intracellular pathways through Cx43 binding proteins[37] or hemichannel formation,[38] thus operating in a GJIC-independent manner.

To further investigate the mechanism of Cx43-induced protection of ARPE-19 cells from oxidative stress, the effect of this stressor on Cx26 was also examined. Given that both Cx43 and Cx26 are active at forming channels, the results provided some support to the premise that channel formation is the key common factor rather than connexin binding proteins, which tend to be different for these connexins. To explore the idea that assembly into functional gap junctions is the feature of importance for protection against oxidative stress, experiments were performed to assess the effect of t-BOOH on cells in which Cx43-specific GJIC or total GJIC was reduced. A naturally occurring human disease-linked mutant of Cx43, G21R, was studied. It is known to exert a dominant-negative effect on coexpressed Cx43[22] and is one of more than 35 mutations associated with the rare autosomal dominant human disorder oculodentodigital dysplasia.[39] In another experiment, Cx43 expression was reduced through an RNAi approach to knock it down.[24] In both cases, the selective downregulation of GJIC by targeting Cx43 resulted in the greater susceptibility of ARPE-19 cells to oxidative damage. In a third approach, pharmacologic reagents were used to inhibit all connexin-based GJIC. Again this resulted in ARPE-19 cells becoming more susceptible to t-BOOH–induced cell death, further confirming that functional connexins protect against oxidative stress-induced injury.

Collectively, these experiments provide evidence for the importance of Cx43 channels in inhibiting oxidative damage, and they strongly argue against a mechanism involving connexin binding proteins. However, the findings do not clearly distinguish between hemichannel function and GJIC. Although dominant-negative, Cx43 knockdown, and pharmacologic agents reduce GJIC, they also affect Cx43 hemichannels.[38,40] Future studies would require an exquisite dissection of hemichannel function from GJIC to further refine the mechanism of Cx43-induced protection to oxidative stress.

In summary, the present study provides evidence that the channel-forming properties of Cx43 mediate protection against cell death induced by acute challenges of t-BOOH in the ARPE-19 cell line of human RPE. Future studies of the maculae of Cx43 knockdown mice and assays of human retinas with and without clinical AMD may provide more insight into this potential mechanism of disease.

Acknowledgments

The authors thank Alex Jian Mao for his assistance.

References

1. Klein R, Wang Q, Klein BEK, Moss SE, Meuer SM. The relationship of age-related maculopathy, cataract and glaucoma to visual acuity. *Invest Ophthalmol Vis Sci*. 1995;36:182–191.
2. Klaver CC, Wolfs RC, Vingerling JR, Hofman A, de Jong PT. Age-specific prevalence and causes of blindness and visual impairment in an older population: the Rotterdam Study. *Arch Ophthalmol*. 1998;116:653–658.
3. The Eye Disease Prevalence Study Group. Prevalence of age-related macular degeneration in the United States. *Arch Ophthalmol*. 2004;122:564–572.
4. Roth F, Bindewald A, Holz FG. Key pathophysiologic pathways in age-related macular degeneration. *Graefe's Arch Clin Exp Ophthalmol*. 2004;242:710–716.
5. Cai J, Nelson KC, Wu M, Sternberg P Jr, Jones DP. Oxidative damage and protection of the RPE. *Prog Ret Eye Res*. 2000;19:205–221.
6. Age-Related Eye Diseases Study Research Group. Risk factors associated with age-related macular degeneration: a case-control study in the age-related eye disease study: Age-Related Eye Disease Study Report Number 3. *Ophthalmology*. 2000;107:2224–2232.
7. Harman D. Aging: a theory based on free radical and radiation chemistry. *J Gerontol*. 1956;11:298–300.
8. Beatty S, Koh HH, Henson D, Boulton M. The role of oxidative stress in the pathogenesis of age-related macular degeneration. *Surv Ophthalmol*. 2000;45:115–134.
9. Tate DJ Jr, Miceli MV, Newsome DA. Phagocytosis and H_2O_2 induce vatalase and metallothionein gene expression in human retinal pigment epithelial cells. *Invest Ophthalmol Vis Sci*. 1995;36:1271–1279.
10. Rozanowska M, Jarvis-Evans J, Korytowski W, Boulton ME, Burke JM, Sarna T. Blue-light induced reactivity of retinal age pigment: in vitro generation of oxygen-reactive species. *J Biol Chem*. 1995;270:18825–18830.
11. Gaillard ER, Atherton SJ, Eldred G, Dillon J. Photophysical studies on human retinal lipofuscin. *Photochem Photobiol*. 1995;61:448–453.
12. Sternberg P Jr, Davidson C, Jones DP, Hagen TM, Reed RL, Drews-Botsch C. Protection of retinal pigment epithelium from oxidative injury by glutathione and pressors. *Invest Ophthalmol Vis Sci*. 1993;34:3661–3668.
13. Cai J, Wu M, Nelson KC, Sternberg P Jr, Jones DP. Oxidant-induced apoptosis in cultured human retinal pigment epithelial cells. *Invest Ophthalmol Vis Sci*. 1999;40:959–966.
14. Bailey TA, Kanuga N, Romero IA, Greenwood J, Luthert PJ, Cheetham ME. Oxidative stress affects the junctional integrity of retinal pigment epithelial cells. *Invest Ophthalmol Vis Sci*. 2004;45:675–684.
15. Goldberg GS, Valiunas V, Brink PR. Selective permeability of gap junction channels. *Biochim Biophys Acta*. 2004;1662:96–101.
16. Upham BL, Kang KS, Cho HY, Trosko JE. Hydrogen peroxide inhibits gap junctional intercellular communication in glutathione sufficient but not deficient cells. *Carcinogenesis*. 1997;18:37–42.
17. Azzam EI, de Toledo SM, Little JB. Direct evidence for the participation of gap junction-mediated intercellular communication in the transmission of damage signals from alpha-particle irradiated to nonirradiated cells. *Proc Natl Acad Sci USA*. 2001;98:473–478.
18. Banrud H, Mikalsen SO, Berg K, Moan J. Effects of ultraviolet radiation on intercellular communication in V79 Chinese hamster fibroblasts. *Carcinogenesis*. 1994;15:233–239.
19. Jordan K, Solan JL, Dominguez M, et al. Trafficking, assembly, and function of a connexin43-green fluorescent protein chimera in live mammalian cells. *Mol Biol Cell*. 1999;10:2033–2050.
20. Thomas T, Telford D, Laird DW. Functional domain mapping and selective trans-dominant effects exhibited by Cx26 disease-causing mutations. *J Biol Chem*. 2004;279:19157–19168.
21. Qin H, Shao Q, Curtis H, et al. Retroviral delivery of connexin genes to human breast tumor cells inhibits in vivo tumor growth by a mechanism that is independent of significant gap junctional intercellular communication. *J Biol Chem*. 2002;277:29132–29138.
22. Roscoe W, Veitch GI, Gong XQ, et al. Oculodentodigital dysplasia-causing connexin43 mutants are non-functional and exhibit dominant effects on wild-type connexin43. *J Biol Chem*. 2005;280:11458–11466.
23. Mao AJ, Bechberger J, Lidington D, Galipeau J, Laird DW, Naus CC. Neuronal differentiation and growth control of neuro-2a cells after retroviral gene delivery of connexin43. *J Biol Chem*. 2000;275:34407–34414.
24. Shao Q, Wang H, McLachlan E, Veitch GI, Laird DW. Down-regulation of Cx43 by retroviral delivery of small interfering RNA promotes an aggressive breast cancer cell phenotype. *Cancer Res*. 2005;65:2705–2711.
25. el-Fouly MH, Trosko JE, Chang CC. Scrape-loading and dye transfer: a rapid and simple technique to study gap junctional intercellular communication. *Exp Cell Res*. 1987;168:422–430.

26. Sia MA, Woodward TL, Turner JD, Laird DW. Quiescent mammary epithelial cells have reduced connexin43 but maintain a high level of gap junction intercellular communication. *Dev Genet*. 1999;24: 111–122.
27. Laird DW, Castillo M, Kasprzak L. Gap junction turnover, intracellular trafficking, and phosphorylation of connexin43 in brefeldin A-treated rat mammary tumor cells. *J Cell Biol*. 1995;131:1193–1203.
28. Woodward TL, Sia MA, Blaschuk OW, Turner JD, Laird DW. Deficient epithelial-fibroblast heterocellular gap junction communication can be overcome by co-culture with an intermediate cell type but not by E-cadherin transgene expression. *J Cell Sci*. 1998;111: 3529–3539.
29. Moore GA, Jewell SA, Bellomo G, Orrenius S. On the relationship between Ca^{2+} efflux and membrane damage during t-butylhydroperoxide metabolism by liver mitochondria. *FEBS Lett*. 1983; 153:289–292.
30. Guan X, Wilson S, Schlenden KL, Ruch RJ. Gap-junction disassembly and connexin 43 dephosphorylation induced by 18 beta-glycyrrhetinic acid. *Mol Carcinog*. 1996;16:157–164.
31. Gögelein H, Dahlem D, Englert HC, Lang HJ. Flufenamic acid, mefenamic acid and niflumic acid inhibit single non-selective cation channels in the rat exocrine pancreas. *FEBS Lett*. 1990;268: 79–82.
32. White M, Aylwin M. Niflumic acid and flufenamic acids are potent reversible blockers of Ca-activated Cl channels in *Xenopus* oocytes. *Mol Pharmacol*. 1990;37:720–724.
33. Srinivas M, Spray DC. Closure of gap junction channels by arylaminobenzoates. *Mol Pharmacol*. 2003;63:1389–1397.
34. Zarbin MA. Current concepts in the pathogenesis of age-related macular degeneration. *Arch Ophthalmol*. 2004;122:598–614.
35. Hanneken A, Lin F-F, Johnson J, Maher P. Flavonoids protect human retinal pigment epithelial cells from oxidative-stress-induced death. *Invest Ophthalmol Vis Sci*. 2006;47:3164–3177.
36. Malfait M, Gomez P, van Veen TA, et al. Effects of hyperglycemia and protein kinase c on connexin43 expression in cultured rat retinal pigment epithelial cells. *J Membr Biol*. 2001;181:31–40.
37. Giepmans BN. Role of connexin43-interacting proteins at gap junctions. *Adv Cardiol*. 2006;42:41–56.
38. Goodenough DA, Paul DL. Beyond the gap: functions of unpaired connexon channels. *Nat Rev Mol Cell Biol*. 2003;4:285–294.
39. Laird DW. Life cycle of connexins in health and disease. *Biochem J*. 2006;394:527–543.
40. Contreras JE, Saez JC, Bukauskas FF, Bennett MV. Gating and regulation of connexin 43 (Cx43) hemichannels. *Proc Natl Acad Sci USA*. 2003;100:11388–11393.